Proceedings of the
8th Graz Brain-Computer Interface Conference 2019 DOI: 10.3217/978-3-85125-682-6-13

EXPECTATION MISMATCH DURING A TRACKING TASK: AN EEG ANALYSIS

M. Bevilacqua [1], C. Lopes-Dias[2], A.I. Sburlea[2], G. Müller-Putz[2]

[1]Defitech Chair in Brain-Machine Interface (CNBI), Center for Neuroprosthetics, School of Engineering, École Polytechnique Fédérale de Lausanne (EPFL), Lausanne, Switzerland
[2]Institute of Neural Engineering (INE), Graz University of Technology, Graz, Austria

E-mail: gernot.mueller@tugraz.at

ABSTRACT: Understanding the dynamics of brain areas' activation during BCI tasks is essential to improve BCIs performance and features selection when training a classifier. The role of the cerebellum in the sudden adaptation of the motor plan in response to unexpected perturbations in tasks with continuous motor control and continuous visual feedback has been well reported in the literature. We recorded EEG data of five subjects to study the cerebellar activation in tasks requiring a sudden motor plan update. Using sLORETA inverse source localization method, we observed activation in the cerebellum at around 200 and 400 ms after the deviation onset. Furthermore, EMG recording and analysis at the level of the neck could disprove that the activity observed was due to movement artifacts.

INTRODUCTION

Being able to precisely localize the components of functional networks involved in a given mental task and knowing the real-time dynamics of brain areas activation can provide a better understanding of the neural processes underlying brain functioning. The information about the temporal interaction between components of different neural networks and their specific role in the processing of mental tasks is essential to obtain a complete comprehension of the brain activity and to be able to decode it precisely. This information could for example be exploited by BCI applications in order to improve the data acquisition, the processing and, above all, the feature extraction process used to train a classifier, increasing the performance of the controlled device [1–3]. EEG provides a temporal resolution in the order of the milliseconds [4]. EEG source localization technique thus represents a potential tool to study almost in real-time the dynamics of neural networks involved in mental tasks. EEG source localization is used mostly to analyze cortical sources formed by groups of pyramidal neuron, since they are thought to be the main contributors to the generation of the electrical potential acquired. However, studies show that it can also be a valid method to investigate sources in the deeper cerebral structures, such as the cerebellum [5–7]. Different studies highlighted the involvement of the cerebellum in continuous performance monitoring [8], in supervised learning during motor tasks [9] and in the adaptation of motor plan in response to visuomotor perturbations [10]. Tseng et al. [10], in a study on goal-directed arm movements, concluded that the adaptation to visuomotor perturbations depends on the cerebellum and that it is driven by the mismatch between predicted and actual sensory outcome of motor commands. EEG evidences of cerebellar role in performance monitoring have been reported by Peterburs et al. [8] and by Wolpert et al. [11], who also hypothesized that in the context of movement coordination, the cerebellum applies an internal forward-model to predict the sensory consequences of actions. Furthermore, the study on the computation method of the cerebellum performed by Doya [9] evidenced that the cerebellum is the specialized organism for supervised learning based on continuous motor tasks with continuous feedback. The results of the reported literature elicited interesting speculations about the cognitive involvement of the cerebellum in tasks with continuous motor control and continuous feedback requiring the adaptation of the motor plan or the need for more control on the motor task. The possible activation of the cerebellum during this type of tasks could indeed be due to an attempt performed by the subject to suddenly adapt the motor plan to an sudden perturbation of the expected task. At the moment of the perturbation onset, the defined target-directed motor plan should be quickly interrupted and updated in order to comply with the new goal; in this framework the cerebellum could be involved in the attempt of adapting the motor plan to the mismatch acknowledged through visual feedback. The hypothesis of the active role of the cerebellum in this framework, if confirmed, could represent a novel finding about the involvement of the cerebellum in expectation mismatch tasks. The aim of this study is thus to use EEG source localization to provide insights about the cerebellar involvement in the processing of continuous motor controlled tasks in which a mismatch between visual feedback and expectation is generated, and a sudden change in the motor plan is required. In addition, this experiment aims to study the involvement of muscle artifacts in the cerebellum activation.

 DOI: 10.3217/978-3-85125-682-6-13

MATERIALS AND METHODS

Hardware and data acquisition: EEG data were recorded at a sampling rate of 1000 Hz using BrainAmp amplifiers and an ActiCap system (Brain Products, Munich, Germany) with 59 active electrodes (FP1, FP2, AF3, AF4, F7, F5, F3, F1, Fz, F2, F4, F6, F8, FT7, FC5, FC3, FC1, FCz, FC2, FC4, FC6, FT8, T7, C5, C3, C1, Cz, C2, C4, C6, T8, TP7, CP5, CP3, CP1, CPz, CP2, CP4, CP6, TP8, P7, P5, P3, P1, Pz, P2, P4, P6, P8, PO7, PO3, POz, PO4, PO8,PO9, O1, Oz, O2, PO10), reference on the right mastoid, the ground electrode in AFz, 3 EOG electrodes (above the nasion and below the outer canthi of the eyes) and 2 EMG electrodes (on the skin, on the left (EMG1) and on the right (EMG2) of the spinal cord; right above the trapezius). EMG recording have been included to the experimental paradigm in order to assess the amplitude of muscular artifacts generated by the movement of the arm and the shoulder during the trials at the level of the neck. In addition to EEG, EOG and EMG channels, one supplementary channel reporting the coordinates of a handle of the joystick used in the experiment was acquired.

Participants and experimental environment: Five volunteers (with ages between 22 and 26 years, 3 male, all right-handed and already experienced in BCI and EEG recording) participated in the experiment, which took place in a darkened shielded room. Participants sat on a comfortable armchair, 1.5 meter away in front of a computer screen displaying the protocol. The right armrest of the chair was replaced by a table with the joystick. EEG data of the 5 subjects were acquired while controlling a cursor on the computer screen with the joystick. The subjects were always able to move the joystick in every direction without dragging the elbow on the table or raising the shoulder.

Experiment overview: The experiment consisted of 10 blocks of 32 trials each. Between each trial there was a 2.5 s break. Between each block the subject could rest as long as wanted, since the beginning of the following block was triggered by pressing a joystick button. 25% of the trials of every block were *deviation* trials, while the resting 75% *no deviation* trials. For all the subjects the exact 3D position of the electrodes on the head was recorded before the beginning of the protocol, using CMS 20 EP system (Zebris Medical GmbH, Isny, Germany). Before the beginning of the protocol, 2 minutes of EEG recording of the subject in a complete resting condition was acquired for every subject.

Trial and task description: As depicted in Figure 1 (top), at the beginning of a trial, 2 equally spaced blue squares were displayed on the upper part of the screen, at the same distance from its center. In addition, a black fixation cross was displayed. On the lower part of the screen there were two circles, one white and one red, vertically aligned. The white circle was automatically moved by the protocol, while the red circle represented the cursor controlled by the subject. The squares, the cross and the two circles were displayed on a grey area, inside which the two circles could move. In each trial, one of the two squares was randomly selected by the protocol as the target, without informing the subject about the decision. The two squares had the same probability to be selected as targets. The subject controlled the cursor through the joystick, and the displacement of the joystick handle was directly proportional to the direction of the movement of the cursor. The task consisted following the white circle with the cursor controlled by the joystick. The white circle was directed towards the target. When the white circle started to move, the subject obtained the control of the cursor and the trial begun. A trial ended when the cursor reached the target defined by the paradigm, when it hit the boundaries of the grey region, or when the time limit of 15 seconds per trial was reached. The subjects were instructed to keep their gaze fixed at the fixation cross and to minimize eye blinking and eye movements.

No deviation trials: In these trials the white circle followed a default trajectory, reaching the center of the target and stopping its movement there (see Figure 1, bottom left). In the presented study, *no deviation* trials have been considered valid only if the participant successfully reached the target. *No deviation* trials that ended because of the cursor hit the boundary of the grey region or the time deadline was reached were not considered in the analysis.

Deviation trials: In these trials, the target changed in the middle of the trial. Therefore, the trajectory of the white circle previously described was subjected to a modification. At the deviation onset, the white circle deviated towards the new target. The new trajectory described an arc of circumference connecting the white circle, at the deviation onset, and the new target. The deviation onset occurred when the white circle was located within the green semicircles depicted in Fig. 1 (top), which were invisible to participants. In *deviation* trials the white circle initially aimed one target, and then deviated to finally reach the other target (see Figure 1, bottom right). Also for *deviation* trials, were considered in the study only the trials that ended with the cursor reaching the final target defined by the white circle.

EEG preprocessing: EEG data was bandpass filtered between 1 and 10 Hz using an IIR Butterworth filter of fourth-order with zero phase. Data was resampled to 250 Hz. EEG, and protocol events were imported on Brainstorm [12] (http://neuroimage.usc.edu/brainstorm). Since individual MRI scans were not available, to every subject was attributed the ICBM152 default anatomy [13]. It has been necessary to define a “virtual onset” for *no deviation* trials ("no deviation onset"), computed as the average of the difference between time of the deviation onset and the start of the *deviation* trial and then added to the starting time of every *no deviation* trial. EEG and EOG data was epoched considering the interval [-700, 1200] ms from deviation and no deviation onset events. Two different types of epochs were thus extracted: *deviation* and *no deviation*. Epochs containing eye blink events were dis-

 DOI: 10.3217/978-3-85125-682-6-13

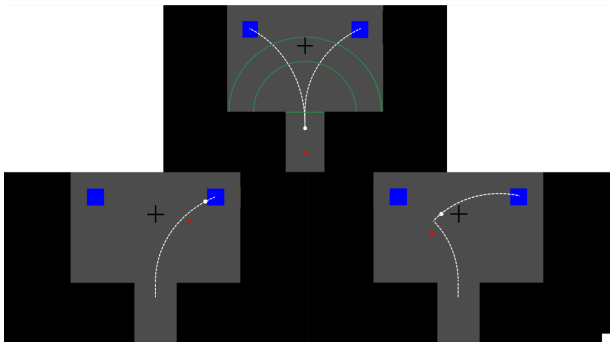

Figure 1: **Top**: starting condition of every trial. Blue squares: fixed targets, white circle: moving target, red circle: controlled cursor, black cross: fixation cross, white lines: default possible trajectories of the moving target (in *no deviation* trials), grey region: area in which the cursor is possible to move, green semicircular lines: area in which a deviation in the trajectory of moving target is possible to occur, green rectilinear line: threshold between upper and lower grey areas. Green and white lines were not visible for the subject during the protocol. **Bottom left**: Moment before a successful end of a *no deviation* trial. **Bottom right**: Moment right after the deviation onset in a *deviation* trial.

carded. On average, the 1% of the trials (*deviation* and *no deviation*) was discarded from every subject. Visual examination of epochs for bad channels was computed, and no channels were removed from any subject.

Joystick coordinates analysis: Together with EEG epochs, also joystick coordinates epochs were extracted. For Subject 1, the acquisition of the joystick coordinates was not available. First, individual averages and then grand averages over 4 subjects of X and Y joystick coordinates have been computed for *deviation* and *no deviation* condition. **Movement Reaction Onset (MRO)**, the time in which the subject reacted to the deviation with a movement of the joystick, has been computed for every subject as the moment in which the derivative of the X coordinate in *deviation* trials changed sign. Then, the average MRO has been computed by averaging the MRO of the four subjects.

EMG analysis: EMG channels were highpass filtered at 1 Hz using an IIR Butterworth filter of fourth-order with zero phase. Also notch filter at 50 Hz was applied to eliminate power line noise. All the frequency information related to muscular artifacts had been kept. EMG channels were resampled to 250 Hz. The moving Root Mean Square (RMS) envelope of EMG channels was then extracted using a time window of 500 ms. Artifact cleaning had been performed using the Signal Space Projection (SSP) method provided by Brainstorm [14]. EMG epochs for *deviation* and *no deviation* conditions were extracted in the same way as EEG and joystick coordinates epochs were.

Scalp level analysis: For every subject, *deviation* and *no deviation* trials were averaged. In order to avoid biases in the SNR (Signal to Noise Ratio) in favor of the condition presenting the highest number of trials (*no deviation*), the same number of epochs were averaged for every condition. The used trials in the *no deviation* condition were chosen from a random uniform distribution from the total number of *no deviation* trials. On average, for every subject, 75 epochs were averaged for both conditions.

Source level analysis: EEG source localization brain imaging was performed with Brainstorm [12]. Since the focus of the source analysis performed was specifically to investigate the source activity at the level of the cerebellum, a *mixed head model* was used to describe the propagation of electrical fields from the cortical surface to the scalp. Cerebral cortex was modeled using a distributed source model, while the cerebellum using an unconstrained distributed model. The ill-posed inverse problem was modeled by means of a distributed source model. Source maps were computed using wMNE (weighted Minimum Norm Estimates) [15] regularization, and normalized according to sLORETA method [16]. The amplitudes of averages for every condition in each subject were normalized by the Global Field Power (GFP) of the baseline period [-600, -100] ms before the event (*deviation/no deviation*) onset. In this way, we normalized the power of the signal across subjects, eliminating the influence of possible inherent higher GFP that could bias the magnitude of source activation. Source analysis on mixed head model was computed on the subject averages of both conditions. Then, grand averages over the 5 subjects were computed at source level for the two conditions. It is important to highlight that the GFP normalization was computed for every subject only on the condition averages, and not on the noise covariance matrix used by sLORETA inverse method. This did not influenced the final source analysis results, but simply scaled in a consistent way the magnitude of the current density of every active source.

RESULTS

EMG analysis: In Fig. 2, the grand averages of the potentials recorded by the two EMG electrodes placed on the neck, for *Deviation* and *No Deviation* conditions are shown. There is no increase in the EMG activity after the cursor deviation onset (black line), neither after the MRO (red dotted line). The only consistent difference is between EMG1 and EMG2, probably because the EMG2 electrode was placed on the right side of neck and the joystick was always moved with the right hand.

Scalp level analysis: Fig. 3 presents the grand averages of the two conditions (*Deviation*/*No Deviation*) at the channels FCz, Cz and Pz. Seven relevant time points have been chosen as a reference in relation with the *Deviation* grand average at FCz: *t=0 ms* (cursor deviation onset), *t=56 ms* (before first small positive deflection), *t=100 ms* (first small positive deflection), *t=168 ms* (negative peak), *t=272 ms* (average MRO), *t=372 ms* (positive peak) and *t=524 ms* (negative deflection after positive peak). The *Deviation* potential shows a negative peak around 168 ms, before the average MRO (red dot-

 DOI: 10.3217/978-3-85125-682-6-13

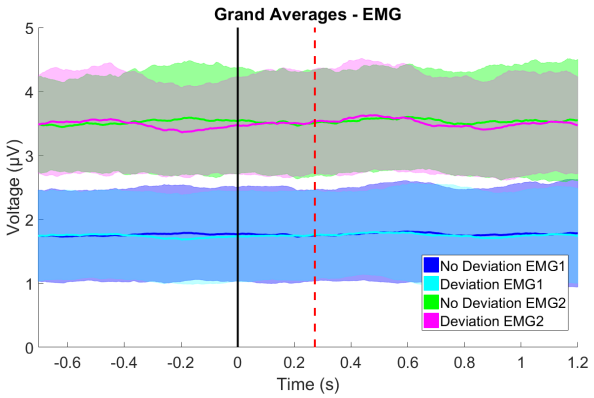

Figure 2: Grand Averages for the 2 conditions (*Deviation*/*No Deviation*) of the 2 EMG channels. The vertical black line represents the time onset of the white circle deviation. The dotted red line represents the average MRO (t=272 ms). The shaded areas indicate the 95% confidence interval for the averaged signals.

ted line), and a positive peak around 372 ms, after the average MRO. *No Deviation* grand average is mostly flat.

Source level analysis: sLORETA source localization inverse method has been computed on the grand averages of the *Deviation* and *No Deviation* trials (Fig. 4). The analysis has been performed on the 7 relevant time points described before. The analysis showed cerebellar activation before (lower, t=168 ms) and after (higher, t=372 ms) the average MRO (t=272 ms). The analysis showed also activation mainly in the pre-SMA (pre-Supplementary Motor Area) during the transition between the two peaks.

DISCUSSION

With this experiment we investigated whether the involvement of cerebellum is present in cognitive processing of expectation mismatch during continuous motor control. The results regarding EMG activation (Fig. 2) did not show noticeable changes after the movement reaction onset of the deviation trials. Therefore, this could disprove the hypothesis that the activation found at the cerebellar level was due to muscular artifacts when handling the joystick. At the scalp level, the shape of the *Deviation* condition grand average resembles the shapes of the most classic error-related potentials (ErrPs) reported in the literature [17–19], with a broad frontocentral negativity at around 200 ms (ERN component) and a broad frontocentral positivity at around 400 ms (Pe component). This can confirm the hypothesis that the potential generated by the expectation mismatch caused by a sudden change in the target-oriented motor plan presents some common features with the ErrPs. The negative peak happened before the reaction movement onset, while the positive one after. Since the Pe component is usually associated with conscious awareness of the expectation mismatch [20, 21], this observation could show that subjects reacted to the deviation before they were consciously aware of it. As expected, grand average of *No deviation* trials appeared almost flat during the entire time interval analyzed. Scalp potential distribution reflected the results provided by literature regarding error-related potential scalp analysis [18, 19]. Source analysis performed on mixed head model with sLORETA inverse method (Fig. 4) confirmed the hypothesis of cerebellum involvement in the processing of expectation mismatches. The cerebellum presented activity in correspondence with the negative and the positive peaks in the deviation condition, while in the interval between the two peaks the pre-SMA and ACC (Anterior Cingulate Cortex) areas appeared more active. This could provide valid insights in relation to the cognitive role of the cerebellum in reinforcement learning, motor performance monitoring and error in continuous motor task. The fact that the cerebellum showed remarkable activation even in correspondence of the negative peak, before the MRO, could confirm the hypothesis that the activity observed was not due to movement artifacts.

CONCLUSION

This study confirmed the possibility of the involvement of cerebellum processing in expectation mismatch tasks with continuous motor control and continuous visual feedback. Furthermore, the hypothesis of the activation being caused by movement artifacts could have been disproved. An open question concerns the activation of the cerebellum in a scenario in which the user is controlling a cursor only through brain signals and without using any muscle activation. It would be interesting to assess if in such a situation the cerebellum would also be involved. Further connectivity studies could be performed on the topic in order to assess the physiological reason underlying the described source activity.

ACKNOWLEDGEMENTS

This work was supported by Horizon 2020 ERC Consolidator Grant 681231 'Feel Your Reach'.

REFERENCES

[1] Goel MK, Chavarriaga R, Millán JdelR. Inverse solutions for brain-computer interfaces: Effects of regularisation on localisation and classification. In: Systems, Man, and Cybernetics (SMC), 2017 IEEE International Conference on. IEEE. 2017, 258–263.
[2] Peralta MRGde, Andino SG, Perez L, Ferrez PW, Millán JdelR. Non-invasive estimation of local field potentials for neuroprosthesis control. Cognitive Processing. 2005;6(1):59–64.
[3] Noirhomme Q, Kitney RI, Macq B. Single-trial EEG source reconstruction for brain–computer interface. IEEE Transactions on Biomedical Engineering. 2008;55(5):1592–1601.
[4] Baillet S, Mosher JC, Leahy RM. Electromagnetic brain mapping. IEEE Signal processing magazine. 2001;18(6):14–30.
[5] Cebolla AM, Petieau M, Dan B, Balazs L, McIntyre

 DOI: 10.3217/978-3-85125-682-6-13

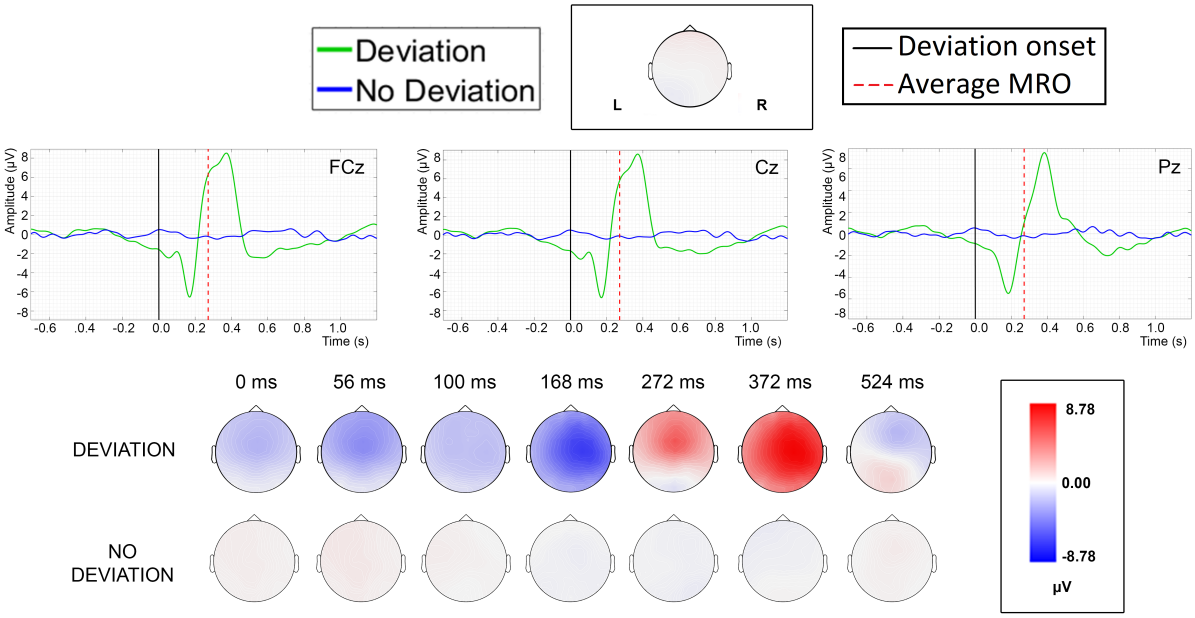

Figure 3: On **top**, the grand averages for the *Deviation* and *No Deviation* conditions at channels FCz, Cz and Pz. The dotted red line is at t=272 ms, and it represents the average MRO. The black continuous line represents the deviation onset. **Below**, the time evolution of scalp distribution of the grand averages for the 2 conditions. The time points t=0 ms, t=56 ms, t=100 ms, t=168 ms, t=272 ms, t=372 ms and t=524 ms are displayed.

J, Cheron G. Cerebellar contribution to visuo-attentional alpha rhythm: insights from weightlessness. Scientific reports. 2016;6:37824.

[6] Attal Y et al. Modeling and detecting deep brain activity with MEG EEG. In: Engineering in Medicine and Biology Society, 2007. EMBS 2007. 29th Annual International Conference of the IEEE. IEEE. 2007, 4937–4940.

[7] Seeber M et al. Subcortical electrophysiological activity is detectable with high-density EEG source imaging. Nature Communications. 2019;10:753.

[8] Peterburs Jutta et al. A cerebellar role in performance monitoring–Evidence from EEG and voxel-based morphometry in patients with cerebellar degenerative disease. Neuropsychologia. 2015;68:139–147.

[9] Doya K. What are the computations of the cerebellum, the basal ganglia and the cerebral cortex? Neural networks. 1999;12(7-8):961–974.

[10] Tseng Y, Diedrichsen J, Krakauer JW, Shadmehr R, Bastian AJ. Sensory prediction errors drive cerebellum-dependent adaptation of reaching. Journal of neurophysiology. 2007;98(1):54–62.

[11] Wolpert DM, Miall RC, Kawato M. Internal models in the cerebellum. Trends in cognitive sciences. 1998;2(9):338–347.

[12] Tadel F, Baillet S, Mosher JC, Pantazis D, Leahy RM. Brainstorm: a userfriendly application for MEG/EEG analysis. Computational intelligence and neuroscience. 2011;2011:8.

[13] Talairach - MRC CBU Imaging Wiki. [Online]. Available: http://imaging.mrccbu.cam.ac.uk/imaging/MniTalairach. [Accessed: 12-Apr-2018].

[14] Uusitalo MA, Ilmoniemi RJ. Signal-space projection method for separating MEG or EEG into components. Medical and Biological Engineering and Computing. 1997;35(2):135–140.

[15] Hämäläinen MS, Ilmoniemi RJ. Interpreting magnetic fields of the brain: minimum norm estimates. Medical biological engineering computing. 1994;32(1):35–42.

[16] Pascual-Marqui RD. Review of methods for solving the EEG inverse problem. International journal of bioelectromagnetism. 1999;1(1):75–86.

[17] Omedes J, Iturrate I, Minguez J, Montesano L. Analysis and asynchronous detection of gradually unfolding errors during monitoring tasks. Journal of neural engineering. 2015;12(5):056001.

[18] Ferrez PW, Millán JdelR. Error-related EEG potentials generated during simulated brain-computer interaction. IEEE transactions on biomedical engineering. 2008;55(3):923–929.

[19] Lopes Dias C, Sburlea AI, Müller-Putz GR. Masked and unmasked error-related potentials during continuous control and feedback. Journal of neural engineering. 2018;15(3):036031.

[20] Overbeek TJM, Nieuwenhuis S, Ridderinkhof KR. Dissociable components of error processing: On the functional significance of the Pe vis-à-vis the ERN/Ne. Journal of Psychophysiology. 2005;19(4):319–329.

[21] Nieuwenhuis S, Ridderinkhof KR, Blom J, Band GPH, Kok A. Error-related brain potentials are differentially related to awareness of response errors: evidence from an antisaccade task. Psychophysiology. 2001;38(5):752–760.

 DOI: 10.3217/978-3-85125-682-6-13

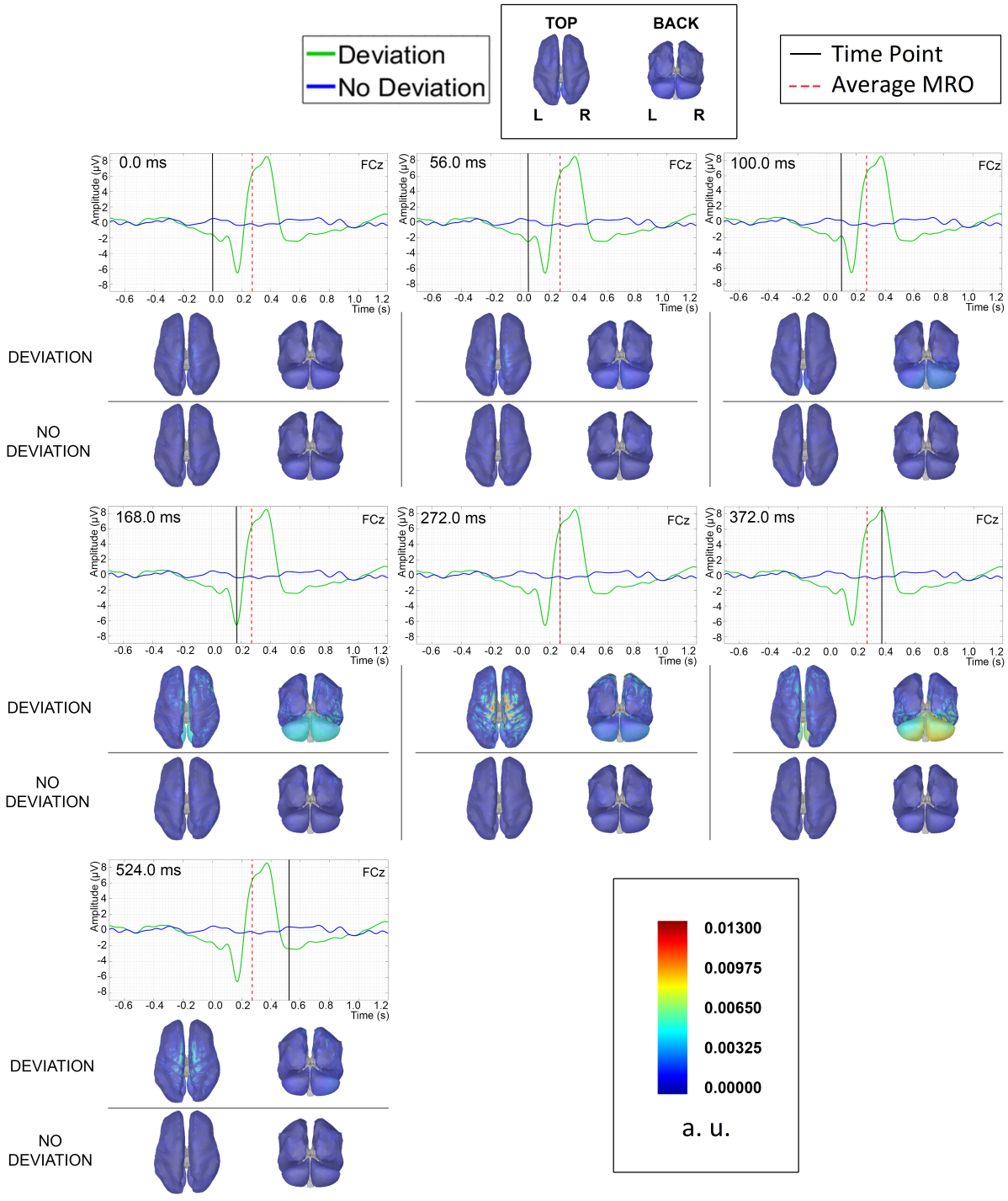

Figure 4: sLORETA source localization computed on the mixed brain surface distributed source model, averaged over the 5 subjects. This mixed brain model includes cerebral cortex and cerebellum surface. Dipoles orientation has been considered constrained to the surface of the cerebral cortex and unconstrained to the cerebellum surface. Seven relevant time points have been taken into account (t=0 ms, t=56 ms, t=100 ms, t=168 ms, t=272 ms, t=372 ms, t=524 ms). For every time point analyzed, the grand averages at channel FCz as been reported as a reference for the cortex views below. The black line indicates the analysed time-points. The dotted red line (t=272 ms) represents the average MRO. Two cerebral and cerebellar cortex surface views for every condition and time point are shown, in this order: top, back. The source activation level on the surfaces is referred to the same scale for all the conditions. The current density of source activation is shown without a unity of measure because of the subject-wise normalization performed before computing the source activity. Nevertheless, this value is proportional to the effective current density.